NOVEL COMPOSITE RIGHT/LEFT-HANDED LEAKY-WAVE ANTENNAS BASED ON THE FOLDED SUBSTRATE-INTEGRATED-WAVEGUIDE STRUCTURES

T. Yang[1, *], P.-L. Chi[2], and R. Xu[1]

[1]Department of Electrical Engineering, University of Electronic Science and Technology of China, Chengdu, China

[2]Department of Electrical Engineering, National Chiao Tung University, Hsinchu, 300 Taiwan

Abstract—In this paper, novel composite right/left-handed (CRLH) leaky-wave antennas based on folded substrate-integrated-waveguide (FSIW) structures are proposed. The proposed leaky-wave antennas were realized by periodically loading the radiating slots on the top metallization of the FSIW-based CRLH transmission lines. The structural advantages of the FSIW combined with the unique dispersion characteristics of the CRLH transmission line enable the proposed leaky-wave antennas to present continuous beam-scanning capability from backfire to endfire directions, occupy smaller footprint size, and provide more design flexibility than the conventional CRLH leaky-wave antennas. Two of such CRLH leaky-wave antennas were developed. In addition to the continuous beam scanning, it is found that the radiation efficiency and polarization of the FSIW-based leaky-wave antennas can be easily tuned by means of the slot size and slot orientation, respectively, indicating their potential for versatile applications. Calculated and experimental results are presented and compared. A good agreement is obtained. To the best of our knowledge, it is the first time that the leaky-wave antenna exploits both of the dispersion behavior of the CRLH transmission lines and the structural benefits of the FSIW configuration.
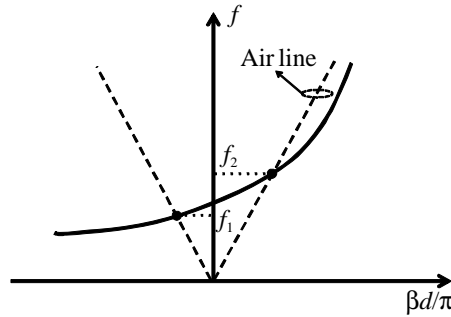
Figure 1. Dispersion diagram of the CRLH transmission line under the balanced condition.

1. INTRODUCTION

Over the last decade, there has been a significant increase of interest in the development of microwave components and systems based on the negative-refractive-index materials [1–3] or the composite right/left-handed (CRLH) transmission-line structures [4]. Numerous CRLH transmission line structures have been proposed to demonstrate the characteristics of the left-handed metamaterials. For Examples, a microstrip-line based CRLH transmission line was proposed in [5], a lumped-element loaded CRLH transmission line was implemented in [6], a fin-line based CRLH transmission line was developed in [7], a split-ring-resonators (SRRs) embedded rectangular waveguide was investigated in [8], a substrate-integrated-waveguide (SIW) based CRLH transmission line was proposed in [9], and so on. Figure 1 shows the dispersion diagram of the CRLH transmission line that is under the balanced condition. In this figure, frequency reange between f_1 and f_2 lies in the fast-wave region where leaky-wave phenomenon takes place [10, 11]. In this region, the propagation constant β varies from the negative to positive values, enabling continuous beam-scanning capability from the backfire to endfire directions. Based on this unique feature, a large number of CRLH leaky-wave antennas have been proposed [9, 12–14]. In the ordinary approach that was used to implement these CRLH leaky-wave antennas, the transmission line parameters, such as the interdigital capacitors in the microstrip line or interdigital slots on the top metallization of the SIW, are not only responsible for the radiation efficiency but also for maintaining the balanced condition. This implies that fewer degrees of deign freedom are applicable to engineer the radiation characteristics as desired [15–

17]. The employment of the newly developed waveguide structure, folded substrate integrated waveguide (FSIW) [18, 19], may provide a good solution to realize the artificial CRLH transmission line for radiated-wave applications with a greater degree of design flexibility. Moreover, while exhibiting identical dispersion property to the SIW, the FSIW has only one-half width of the SIW counterpart and thus is beneficial for size reduction.

In this paper, two novel CRLH leaky-wave antennas based on the FSIW structures are implemented experimentally. In addition to demonstrating continuous beam-scanning ability, the proposed antennas are size reduced and can be controlled or adapted easily to meet the desired radiation specifications when compared to the CRLH leaky-wave antennas published previously. Measured and simulated results are provided and discussed in details. Good agreement is achieved. To the best of the authors' knowledge, the proposed leaky-wave antennas are the first implementations of the CRLH leaky-wave antennas based on the FSIW structures.

2. THE PROPOSED ANTENNA UNIT CELL BASED ON THE FSIW

Figure 2(a) shows 3D configuration of the unit cell in the proposed CRLH leaky-wave antenna based on the FSIW. For each unit cell, a slot is created on the top metal plane of the FSIW-based CRLH transmission line and is used to leak the microwave energy for radiation purpose. The middle metal plane has interdigital fingers in the center
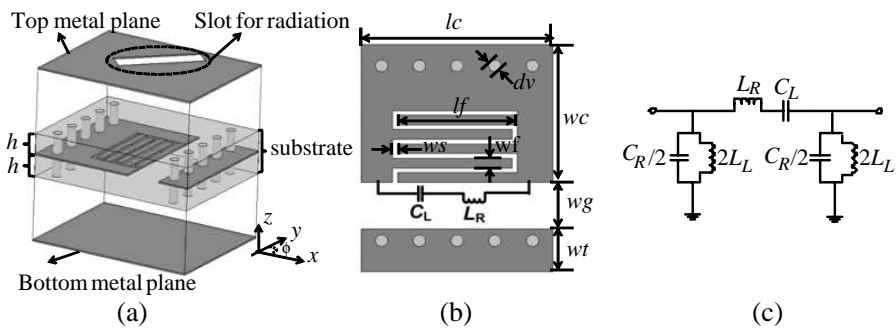

Figure 2. (a) 3D view of the unit cell for the proposed CRLH Leaky-wave antenna based on the FSIW. (b) Top view of the middle metal plane of the unit cell. (c) Equivalent circuit model for the proposed unit cell.

and is connected to the top and bottom metal planes through the metallic vias on both sides, as shown in Figure 2(b). Referring to the equivalent circuit model of the CRLH unit cell in Figure 2(c), the interdigital fingers contribute to the right-handed inductance (L_R), and the slots between the interdigital fingers give rise to the left-handed capacitance (C_L). Furthermore, the left-handed inductance (L_L) comes from the metallic vias that connect the middle metal plane (signal layer) to the top/bottom planes (ground planes), and the right-handed capacitance (C_R) results from the capacitance developed between the middle metal plane and the top/bottom metal planes.

Based on the equivalent circuit model in Figure 2(c), the dispersion relation can be obtained from the following equation [4],

$$\beta = \frac{1}{d} \cos^{-1}\left[1 - \frac{\omega^2}{2\omega_R^2} - \frac{\omega_L^2}{2\omega^2} + \left(\frac{1}{\omega_{sh}^2} + \frac{1}{\omega_{se}^2} \right) \frac{\omega_L^2}{2} \right] \qquad (1)$$

where ω_{sh} and ω_{se} represent the shunt and series resonant frequencies, respectively, and are given as follows

$$\omega_{sh} = \frac{1}{\sqrt{C_R L_L}} = 2\pi f_{sh}, \quad \omega_{se} = \frac{1}{\sqrt{C_L L_R}} = 2\pi f_{se}, \qquad (2)$$

Furthermore, ω_R and ω_L are given as follows,

$$\omega_R = \frac{1}{\sqrt{C_R L_R}} = 2\pi f_R, \quad \omega_L = \frac{1}{\sqrt{C_L L_L}} = 2\pi f_L \qquad (3)$$

To obtain the dispersion characteristics of the proposed unit cell, the periodic boundary condition is applied to the proposed unit cell and the unit cell is simulated in the full-wave EM simulator, the Ansoft HFSS 12. The calculated dispersion diagram is shown in Figure 3. Note that the simulated result is based on the substrate of Rogers 5880 of dielectric constant of 2.2 and thickness of 0.508 mm, and the dimension of the unit cell is shown in Table 1. From the dispersion curve, the left-handed property is observed from 4.5 GHz to 5.6 GHz as the phase velocity is antiparallel to the group velocity. From 5.6 GHz to 7.5 GHz, on the other hand, the right-handed property takes place where the phase velocity is parallel to the group velocity. Particularly, the leaky-wave radiation phenomenon develops from 4.8 GHz to 6.5 GHz where a CRLH antenna can be implemented by cascading the proposed unit cells.

Since the radiation originates from the slot on the top metallization of the FSIW structure, the slot size determines the strength of the radiation leakage. By controlling the slot size of the unit cell, the amount of the leakage or the radiation efficiency can be easily tuned. The leakage factor, Ra, from the slot can be calculated as follows;
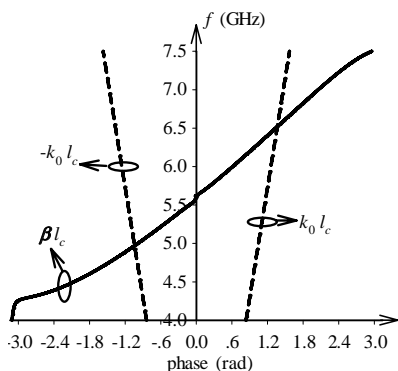
$$Ra = 1 - |S(1,1)|^2 - |S(2,1)|^2 \qquad (4)$$

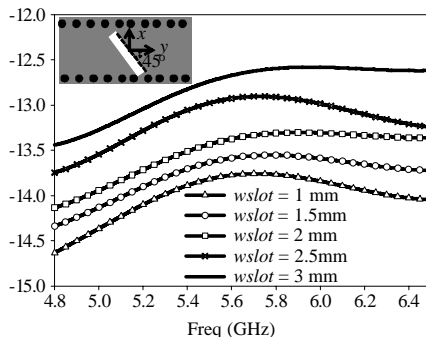**Figure 3.** The dispersion diagram for the proposed slotted unit cell.

Figure 4. The amount of the leakage versus the slot width for one unit cell.

assuming that the dielectric and conductors are lossless and that the via walls on both sides are replaced by solid metal walls. The investigation of the leakage amount from a unit cell with respect to the slot width *wslot* is shown in Figure 4. It should be noted that the slot with a rotation of 45° with respect to the *y*-axis is considered in this case. As observed, the amount of the leakage increases with the slot as expected. Moreover, the amount of leakage shows similar dependence on the slot length, which is not included here. This leakage-controllable property facilitates design of the desired radiation-aperture distribution such as Taylor distribution along the leaky-wave antenna so as to obtain high directive beam with very low side-lobe level [15–17]. It should be noted that, in the conventional implementation of the CRLH leaky-wave antennas, the radiation capability is directly associated with the CRLH transmission-line parameters that have to fulfill transmission-line requirements, such as the balanced condition. Therefore, the radiation efficiency cannot be easily tuned without affecting the transmission line properties.

In addition to a greater freedom of design flexibility for the effective radiation aperture, the proposed leaky-wave antenna offers

Table 1. The physical dimensions of the simulated unit cell. Unit: mm.

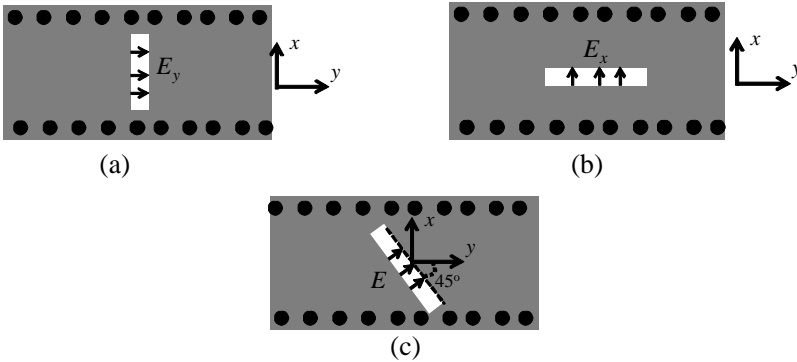| lc	lf	wc	dv	wf	wg	ws	wt	$wslot$	$lslot$	h
7.52	5.1	7.4	0.6	0.5	3.4	0.22	1	2	8.1	0.508

Figure 5. Three general arrangements of the radiating slots. (a) The transverse slot, (b) the longitudinal slot, and (c) the 45°-directed slot.

the benefit of antenna polarization agility by varying the orientation of the slot. In Figure 2(a), the orientation of the slot can be in arbitrary direction. Assuming that the width of the slot is much smaller than its length, the electric field over the aperture of the waveguide will be dominated by the component in the direction parallel to the shorter edges of the slot [20–24]. Three different slot orientations, including the transverse, longitudinal, and 45°-directed (with respect to the longitudinal direction) slots, are illustrated in Figure 5. When the slots are transversely and longitudinally arranged as shown in Figures 5(a) and (b), respectively, the dominant electric field over the aperture will be E_y and E_x, respectively. On the other hand, when the slot is 45° clockwise rotated from the longitudinal case, as shown in Figure 5(c), the electric field will point to the 45° direction with respect to the longitudinal direction of the antenna structure. As a result, the antenna polarization, which is parallel to the electric field distribution over the aperture, can be easily engineered by controlling the orientation of the slots on the proposed antenna structure. This advantage lends the proposed CRLH antenna structure to the application of the polarization diversity, as was demonstrated in the conventional SIW leaky-wave antennas [25].

3. SIMULATION AND EXPERIMENTAL RESULTS

To validate our idea, a CRLH leaky-wave antenna composed of 15 aforementioned unit cells was developed and characterized. The proposed antenna consists of the two layers of the Rogers 5880 substrates with the dielectric constant of 2.2 and thickness of 0.508 mm,
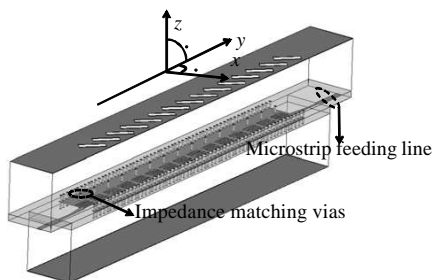
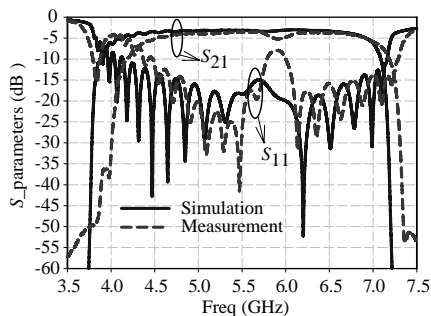**Figure 6.** The proposed CRLH leaky-wave antenna based on the FSIW.

Figure 7. Simulated and measured S-parameters for the proposed leaky-wave antenna.

as shown in Figure 6. Note that the lower substrate is shorter than the upper one in order to facilitate the feed excitation using the $50\,\Omega$ microstrip lines at both ends. The slots of the same size are periodically located on the top metal plane and are arranged at $45°$ with respect to the longitudinal or propagation direction of the transmission line, as the case in Figure 5(c). In addition, in order to improve the impedance matching, an array of impedance-matching vias is inserted near the slots as was proposed in [23, 26], and an optimization process is used to maintain the balance condition.

The simulated and measured S-parameters for the proposed antenna with 15 unit cells are shown in Figure 7. The simulation results were derived from the Ansoft HFSS. A good agreement between the simulated and measured results is obtained. The passband shift is observed in the measurement, and meanwhile a small impedance-mismatch region is found around $5.9\,\mathrm{GHz}$ where impedance matching is maintained and designed as the transition frequency of the CRLH transmission line in the simulation. These discrepancies are mainly attributed to the fabrication errors from the antenna assembly in which a thin glue film is used to stack two layers of substrates. The difficulty in precise modeling of the thickness and electrical properties of the glue film leads to the deviation between the simulated and measured results. The measured insertion loss is around $-4\,\mathrm{dB}$ in the passband. In addition, the band ranging from $4\,\mathrm{GHz}$ to $5.9\,\mathrm{GHz}$ corresponds to the left-handed region while the right-handed region starts from $5.9\,\mathrm{GHz}$ to $7\,\mathrm{GHz}$, which was inferred from the transient electric-field distribution shown in Figure 8. In Figure 8(a), at $4.6\,\mathrm{GHz}$, the transient electric-field distribution along the antenna shows the backward-wave propagation in the structure. The electric field distribution at $5.8\,\mathrm{GHz}$,
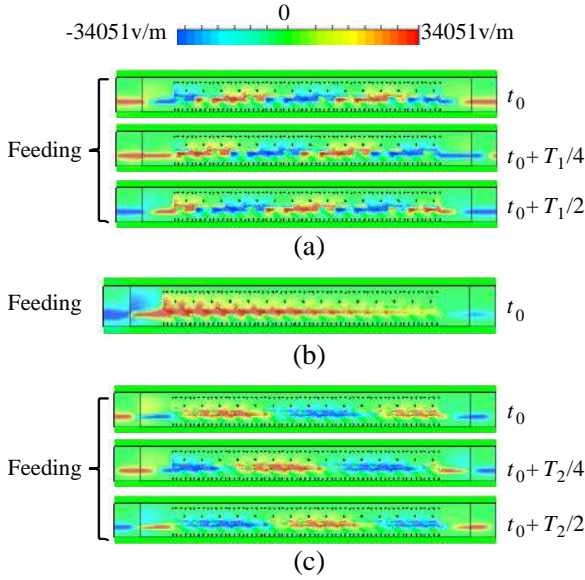
Figure 8. Illustrations of the transient electric field distribution (from CST Microwave Studio) over the proposed CRLH leaky-wave antenna at different frequencies. The initial time $t_0 = 0.2$ ns. (a) Transient electric field at $f_1 = 1/T_1 = 4.6$ GHz, (b) transient electric field at $f_0 = 5.8$ GHz, and (c) transient electric field at $f_2 = 1/T_2 = 6.4$ GHz.
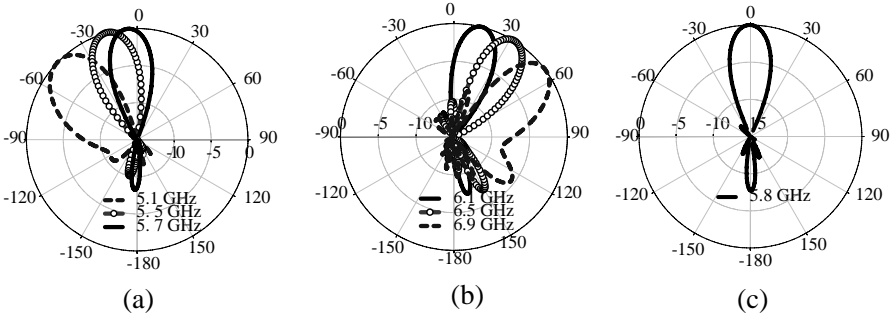

Figure 9. Simulated radiation patterns at different frequencies for the proposed leaky-wave antenna with 15 unit cells. (a) Radiation patterns in the left-handed region. (b) Radiation patterns in the right-handed region. (c) Radiation pattern at the transition frequency.

as shown in Figure 8(b), shows a nearly constant field distribution, indicating the infinite wavelength propagation. Figure 8(c) plots the electric field distribution at 6.4 GHz where the forward propagation
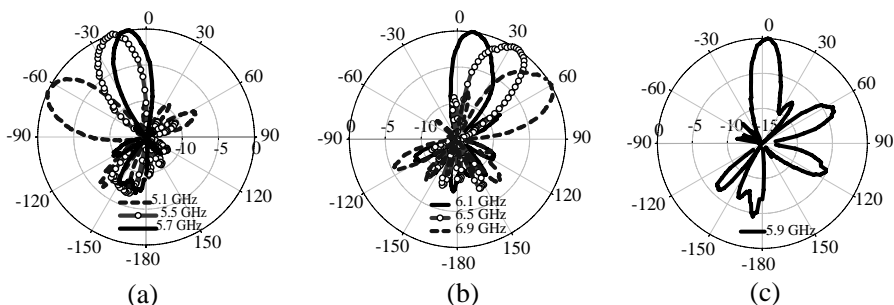
Figure 10. Measured radiation patterns at different frequencies for the proposed leaky-wave antenna with 15 unit cells. (a) Radiation patterns in the left-handed region. (b) Radiation patterns in the right-handed region. (c) Radiation pattern at the transition frequency.

phenomenon is clearly observed. Furthermore, the simulated and measured radiation patterns in the principal plane ($\varphi = 90°$) shown in Figures 9 and 10, respectively, confirm our observation in the transient-field distributions. The continuous beam-scanning from backfire to end-fire directions is clearly. The main beam scans from $\theta = -65°$ to $\theta = +58°$ as the frequency varies from 5.1 GHz to 6.9 GHz in the experiments, whereas the main beam scans from $\theta = -50°$ to $\theta = +55°$ in the simulations. The broadside radiation occurs at 5.9 GHz in the measurement while it was observed at 5.8 GHz in the simulation. The discrepancy is due to the frequency shift observed from the experimental results as shown in Figure 7. It is noted that the frequency for broadside radiation at 5.8 GHz here is slight higher than the frequency of 5.6 GHz for $\beta = 0$ in the dispersion diagram of Figure 3. The discrepancy is due to the added impedance matching vias in Figure 6 for cancelling the mutual coupling between different radiation slots. These added impedance matching vias act as shunt inductance and will decrease the left-handed inductance L_L in Figure 2(c). Thus, the frequency for $\beta = 0$ will shift higher, resulting higher broadside radiation frequency.

Figure 11 compares the simulated and measured gains. While the average gain in the entire scanning range is around 1 dB in the simulation, the measured gain is around -1 dBi except the gain obtained at the transition frequency of 5.9 GHz. The discrepancy between the simulated gain and measured gain may be due to three factors. Firstly, the metallic traces of the antenna are set to be perfect conduct sheets in simulation to reduce the complexity of simulation structure, thus, the conduct loss of the antenna is not included in

the simulation. Secondly, the real dielectric loss of the substrate and glue layer may be higher than the simulation cases where the dielectric loss tangents are all set to be 0.0009. Thirdly, the losses or reflections introduced by the cable and connectors in measurement are not considered in the simulation. All these factors contribute to the discrepancy between the simulated and measured gain. The measured gain at 5.9 GHz is about -4 dBi that is much lower than the gain at other frequencies. This decreased gain at 5.9 GHz is attributed to the presence of the impedance-mismatching, as was discussed in Figure 7.

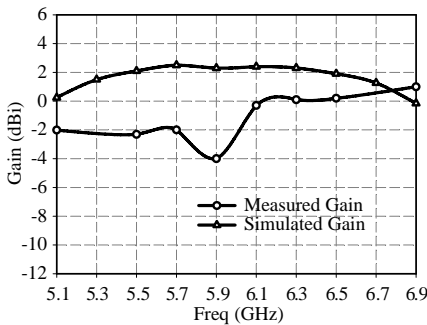In addition, from Figure 7, it is found that the $|S_{21}|$ is around

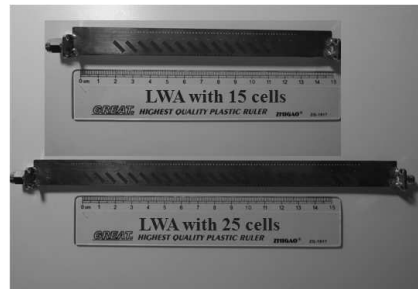**Figure 11.** Simulated and measured gains of the leaky-wave antenna with 15 unit cells.

Figure 12. Photographs of the fabricated leaky-wave antennas. Upper antenna is of 15 unit cells while the lower antenna is of 25 unit cells.
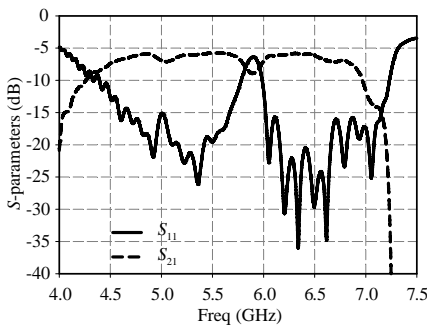

Figure 13. Measured S-parameters for the proposed leaky-wave antenna with 25 unit cells.
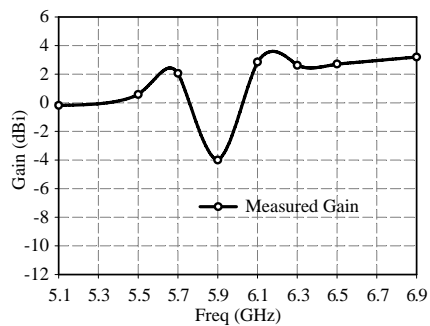

Figure 14. easured gains of the proposed leaky-wave antenna with 25 unit cells.

−4 dB, which indicates that a considerable portion of the power is left in the transmission line and absorbed by the termination at the other end. This explains the relatively low gain measured in Figure 11. In order to increase the antenna gain, more unit cells can be cascaded to leak out the remaining power when wave propagates along the transmission line. To validate this concept, 10 more unit cells are added to the original antenna with 15 cells. Photographs of both fabricated antennas are shown in Figure 12. The physical size of the antenna with 15 unit cells is 144.8 mm × 15 mm × 1.016 mm, while the antenna with 25 unit cells is 212 mm × 15 mm × 1.016 mm.

Figure 13 gives the measured S-parameters for the fabricated antenna with 25 unit cells. The impedance-mismatching region around 5.9 GHz is observed as well. Except this region, the measured $|S_{11}|$ from 4.5 GHz to 7 GHz is below −10 dB, meaning that the antenna is well matched. The $|S_{21}|$ in the entire operating band of interest is around −6 dB, that is 2 dB lower than the previous case of the leaky-wave antenna with 15 unit cells. This provides the improved radiation efficiency for the newly constructed antenna. Figure 14 plots the measured gains for the antenna with 25 unit cells. As observed, the measured gains are averagely 2-dB increased in the frequency scanning range as compared to those obtained for the first antenna. The antenna gain can be enhanced further by cascading more unit cells, and the beam width or directivity can be thus improved further. The measured radiation patterns for the leaky-wave antenna with 25 unit cells are shown in Figure 15. Similar to the first antenna, the beam-scanning phenomenon is clearly observed where the main beam moves
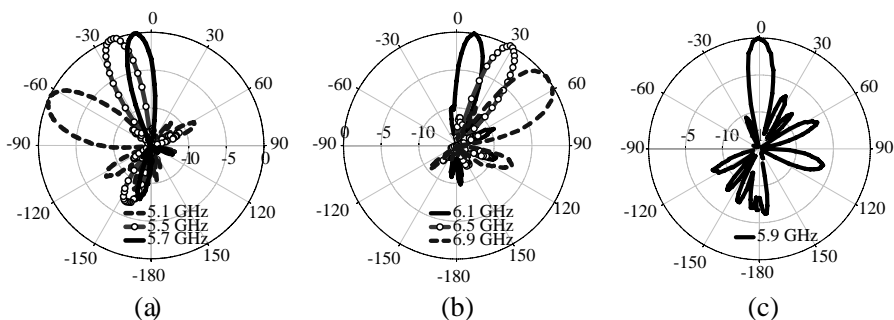

Figure 15. Measured radiation patterns at different frequencies for the leaky-wave antenna with 25 unit cells. (a) Radiation patterns in the left-handed region. (b) Radiation patterns in the right-handed region. (c) Radiation pattern at the transition frequency.

from $\theta = -65°$ to $\theta = +58°$ as the frequency varies from 5.1 GHz to 6.9 GHz. The broadside radiation takes place at 5.9 GHz. As compared to the first antenna, the antenna with 25 unit cells has much narrower beam width, and its 3-dB beamwidths at 5.1 GHz, 5.5 GHz, 5.7 GHz, 5.9 GHz, 6.1 GHz, 6.5 GHz, and 6.9 GHz are 25°, 16.27°, 14.63°, 15°, 14.01°, 15.3°, and 28.68°, respectively.

4. CONCLUSION

In this paper, novel CRLH leaky-wave antennas based on the FSIW are designed, fabricated, and tested. The proposed leaky-wave antenna prototype can be easily engineered to increase the effective radiation aperture or present the specific polarization of interest, both of which overcome the major disadvantages observed in the traditional realizations. The calculated and experimental results are provided and compared. A good agreement is achieved.

REFERENCES

1. Shelby, R. A., D. R. Smith, and S. Schultz, "Experimental verification of a negative index of refraction," *Science*, Vol. 292, No. 5514, 77–79, 2001.

2. Oliner, A. A., "A periodic-structure negative-refractive-index medium without resonant elements," *IEEE AP-S/URSI Int. Symp.*, Vol. 41, Jun. 16–21, 2002.

3. Elefttheriades, G. V. and K. G. Balmain, *Negative Refraction Metamaterials: Fundamental Properties and Applications*, John Wiley & Sons, 2005.

4. Caloz, C. and T. Itoh, *Electromagnetic Metamaterials*, Wiley, New York, 2005.

5. Caloz, C. and T. Itoh, "Transmission line approach of left-handed (LH) materials and microstrip implementation of an artificial LH transmission line," *IEEE Trans. Antennas Propag.*, Vol. 52, No. 5, 1159–1166, May 2004.

6. Eleftheriades, G. V., A. K. Iyer, and P. C. Kremer, "Planar negative refractive index media using periodically L-C loaded transmission lines," *IEEE Trans. Microw. Theory Tech.*, Vol. 50, No. 12, 2702–2712, Dec. 2002.

7. Decoopman, T., A. Marteau, E. Lheurette, O. Vanbesien, and D. Lippens, "Left-handed electromagnetic properties of split-ring resonator and wire loaded transmission line in a fin-line

technology," *IEEE Trans. Microw. Theory Tech.*, Vol. 54, No. 4, 1451–1457, Apr. 2006.

8. Hrabar, S., J. Bartolic, and Z. Sipus, "Waveguide miniaturization using uniaxial negative permeability metamaterial," *IEEE Trans. Antennas Propag.*, Vol. 53, No. 1, 110–119, Jan. 2005.

9. Dong, Y. D. and T. Itoh, "Composite right/left-handed substrate integrated waveguide leaky-wave antennas," *39th Eur. Microw. Conf.*, 276–279, 2009.

10. Ishimaru, A., *Electromagnetic Wave Propagation, Radiation, and Scattering*, Prentice Hall, 1991.

11. Oliner, A., "Chapter leaky-wave antennas," *Antenna Engineering Handbook*, R. C. Johnson Ed., 3rd Edition, McGraw Hill, New York, 1993.

12. Lim, S., C. Caloz, and T. Itoh, "Electronically scanned composite right/left handed microstrip leaky-wave antenna," *IEEE Microw. Wireless Compon. Lett.*, Vol. 14, No. 6, 277–279, Jun. 2004.

13. Lim, S., C. Caloz, and T. Itoh, "Metamaterial-based electronically controlled transmission-line structure as a novel leaky-wave antenna with tunable radiation angle and beamwidth" *IEEE Trans. Microw. Theory Tech.*, Vol. 53, No. 1, 161–173, Jan. 2005.

14. Casares-Miranda, F. P., C. Camacho-Penalosa, and C. Caloz, "High-gain active composite right/left-handed leaky-wave antenna," *IEEE Trans. Antennas Propag.*, Vol. 54, No. 8, 2292–2300, Aug. 2006.

15. Yang, N., C. Caloz, and K. Wu, "Full-space scanning periodic phase-reversal leaky-wave antenna," *IEEE Trans. Microw Theory Tech.*, Vol. 58, No. 10, 2619–2632, Oct. 2010.

16. Cheng, Y. J., W. Hong, K. Wu, and Y. Fan, "Millimeter-wave substrate integrated waveguide long slot leaky-wave antennas and two-dimensional multibeam applications," *IEEE Trans. Antennas Propag.*, Vol. 59, No. 1, 40–47, Jan. 2011.

17. Chen, P., W. Hong, Z. Kuai, and J. Xu, "A substrate integrated waveguide circular polarized slot radiator and its linear array," *IEEE Antennas Wireless Propagat. Lett.*, Vol. 8, 120–123, 2009.

18. Zhai, G. H., W. Hong, K. Wu, J. X. Chen, P. Chen, J. Wei, and H. J. Tang, "Folded half mode substrate integrated waveguide 3 dB coupler," *IEEE Microw. Wireless Compon. Lett.*, Vol. 18, No. 8, 101–103, Feb. 2008.

19. Che, W., L. Geng, K. Deng, and Y.-L. Chow, "Analysis and experiments of compact folded substrate-integrated waveguide," *IEEE Trans. Microw. Theory Tech.*, Vol. 56, No. 1, 88–93,

Jan. 2008.

20. Josefsson, L. G., "Analysis of longitudinal slots in rectangular waveguides," *IEEE Trans. Antennas Propag.*, Vol. 35, No. 12, 1351–1357, Dec. 1987.

21. Joseffsson, L., "A waveguide transverse slot for array applications," *IEEE Trans. Antennas Propag.*, Vol. 41, No. 7, 1351–1357, Jul. 1993.

22. Elliott, R. S., "An improved design procedure for small arrays of shunt slots," *IEEE Trans. Antennas Propag.*, Vol. 31, No. 1, 48–53, Jan. 1983.

23. Park, S., Y. Okajima, J. Hirokawa, and M. Ando, "A slotted post-wall waveguide array with interdigital structure for 45° linear and dual polarization," *IEEE Trans. Antennas Propag.*, Vol. 53, No. 9, 2865–2871, Sep. 2005.

24. Kim, D.-Y., W. Chung, C. Park, S. Lee and S. Nam, "Design of a 45°-inclined SIW resonant series slot array antenna for Ka-band," *IEEE Antennas and Wireless Propag. Lett.*, Vol. 10, 2011.

25. Chen, Y. J., W. Hong, and K. Wu, "Millimeter-wave half mode substrate integrated waveguide frequency scanning antenna with quadric-polarization," *IEEE Trans. Antennas Propag.*, Vol. 58, No. 6, 1848–1855, Jun. 2010.

26. Park, S., J. Hirokawa, and M. Ando, "Simple analysis of a slot with a reflection-canceling post in a rectangular waveguide using only the axial uniform currents on the post surface," *IEICE Trans. Commun.*, Vol. E86-B, No. 8, 2482–2487, Aug. 2003.